

VARIABLE STARS IN THE FIELD OF THE GLOBULAR CLUSTER NGC 3201

KASPAR VON BRAUN
University of Michigan
Department of Astronomy
500 Church
Ann Arbor, MI 48109-1090
kaspar@astro.lsa.umich.edu

AND

MARIO MATEO
University of Michigan
Department of Astronomy
500 Church
Ann Arbor, MI 48109-1090
mateo@astro.lsa.umich.edu
Draft version November 5, 2018

ABSTRACT

We report on the discovery and analysis of 14 short-period variable stars in the field of the southern globular cluster NGC 3201, located within roughly two magnitudes on either side of the main-sequence turnoff. 11 of these variable stars are eclipsing binaries, one is an RR Lyrae, and two are thus far unclassified systems. Among the eclipsing binary stars, nine are of the W Ursa Majoris (W UMa) type, one an Algol (EA) system, and one a detached system. Using spectroscopic follow-up observations as well as analysis of the variables' locations in the color-magnitude diagram of the cluster, we find that only one variable star (a W UMa type blue straggler) is actually a member of NGC 3201. We present the phased photometry lightcurves for all the variable star systems as well as their locations in the field-of-view and in the color-magnitude diagram.

Subject headings: Globular Clusters: individual (NGC 3201); color-magnitude diagrams; dust, extinction; binaries: eclipsing; blue stragglers; stars: variable: general.

1. INTRODUCTION

Variable stars have historically served as important tools and “laboratories” in our understanding of star formation, the formation of stellar clusters, the calibration of distance determination methods, and a variety of other areas. In particular, the study of eclipsing binary stars (EBs) in a globular clusters (GC) can provide a method of examining certain aspects of the GC itself, and it may be used to obtain a value for the cluster’s distance and a constraint concerning turnoff masses of the GC stars (see, e.g., Paczynski (1996)).

Simply detecting EBs in the fields of GCs and confirming cluster membership is a straightforward - though data-intensive - task. These systems expand the relatively meager sample of EBs which are currently confirmed GC members (see for example Mateo (1996); McVean et al. (1997); Rubenstein (1997); Rucinski (2000), and references therein). A statistical evaluation of the number of known member EBs in GCs can help in the determination of physical quantities such as the binary frequency in GCs as a parameter in the study of dynamical evolution of GCs (see for example Hut et al. (1992)), or in the calibration of methods such as the Rucinski magnitudes of and corresponding distances to W UMa binaries (see Section 4.3, and Rucinski (1994, 1995, 2000)).

Moreover, the detection of blue straggler (BS) binary systems would assist in shedding light on the binary frequency among this subclass of stars, which, in turn, could

help understand their formation and evolution. Some hypotheses in the study of the formation of blue stragglers claim that they have formed by collisions between single stars, coalescence of binary systems, and/or interactions between binary systems. Getting a handle on the frequency of binary blue stragglers in a certain GC would therefore present a tool for probing into the dynamical past and even the star formation history of the GC itself (see for example Leonard & Linnell (1992); Hut (1993); Livio (1993); Sills & Bailyn (1999); Sills et al. (2000)).

The simultaneous analysis of photometric and spectroscopic data for individual EB systems can provide a direct estimate of the distance to the system (see for example Andersen (1991) and Paczynski (1996)), and thus, if the EB is a GC member, to the GC itself. The main sources of error in the distance determination are a) the relation between surface brightness and effective temperature of the binary and b) the precise determination of the interstellar reddening along the line of sight to the EB. The method itself, however, is free of intermediate calibration steps and can provide direct distances out to tens of kpc. In turn, the knowledge of the distances to GCs can then be used to calibrate a variety of other methods, such as the relation between luminosity and metallicity for RR Lyrae stars.

The very same analysis can, in principle, be used to obtain the Population II masses of the individual components of the EB system (see Paczynski 1996). If mass is conserved, the evolution of any EB may be expressed by

$M_1 + M_2 = M_{1,0} + M_{2,0} + M_L$, where M_i are the present day masses of the two components, $M_{i,0}$ are their initial masses, and M_L is the total mass loss from the system. If one assumes that $M_L = 0$ (no mass loss), then the difference between present day masses and initial masses of the components is only due to the mass transfer history between the two stars. This demonstrates the value of detecting *unevolved* EB systems. These are systems where the binary components are detached, no mass transfer has taken place, and the present day masses are therefore equal to the initial masses.

A direct determination of the ages of the systems, however, remains a challenging task. The reasons for this are described in Paczynski (1996); we will briefly repeat them here. Analysis of various theoretical isochrones (e.g., Bertelli et al. (1994), D. VandenBerg 2000, private communication; based on evolutionary models by VandenBerg et al. (2000)) readily shows that at the main-sequence turnoff,

$$age_{MSTO} \sim Lum_{MSTO}^{-1} \sim Mass_{MSTO}^{-3.7}. \quad (1)$$

From Kepler's third law, it is apparent that $M_1 \sim K_2^3$, where M_1 is the mass of the first component and K_2 is the radial velocity amplitude of the second component. Combining these two relations gives $age_{MSTO} \sim K^{11}$, implying a 12% uncertainty in age for a 1% uncertainty in the velocity amplitude! A perhaps more rewarding approach would therefore be to use the MSTO masses to provide a fundamental check of stellar models at low [Fe/H]. In order to do this, one needs to either detect detached EB systems (and assume no mass loss, in which case the zero-age masses equal the MSTO masses of the two components), or reconstruct the history of mass transfer between contact EBs to obtain zero-age masses for the two stars.

We are currently undertaking a survey of approximately 10 Galactic GCs with the aim of identifying photometrically variable EBs around or below the MSTO. Our observing strategy, aimed at detecting binaries in the period range of approximately 0.2 to 5 days (see Hut et al. (1992)) basically consists of repeated observations of a set of GCs during each night. Multiple observing runs are usually helpful in detecting variables with a period of close to one day (or to a multiple thereof). The more valuable detached systems are generally much harder to detect because a) they will eclipse each other only within a small range of inclination angles due to the larger distances between the components, b) their duty cycle¹ is very low, and c) they vary less in brightness (if at all) inbetween eclipses than the more distorted components of contact systems. Fairly extensive coverage is therefore usually needed in order to detect detached EB systems.

NGC 3201, by chance one of the first GCs in our sample that we analyzed, has been probed for the existence of binary stars in the past, most recently by Côté et al. (1994). The results of even earlier work on variables in NGC 3201 are summarized in Sawyer-Hogg (1973) and Clement et al. (2001), and references therein. The magnitude and period ranges of the EBs covered in these earlier studies, however,

¹ The duty cycle of an EB is defined as the fraction of the orbital period during which the system is experiencing an eclipse for an edge-on system (inclination angle $i = 90^\circ$).

² IRAF is distributed by the National Optical Astronomy Observatories, which are operated by the Association of Universities for Research in Astronomy, Inc, under cooperative agreement with the NSF.

does not overlap with the work presented here.

Details on our photometry observations are given in Section 2. We then describe how we detect variable stars in our sample and determine their periods in Section 3. These two Sections set out the methods we will use for the other clusters in our sample. Section 4.1 contains our results concerning the locations of the binaries in the field as well as in the CMD of NGC 3201. In Section 4.2, we present the phased lightcurves for all the variable stars we find. We calculate distance moduli to our set of W UMa type EBs using Rucinski's formula (Rucinski 1994, 1995, 2000) in Section 4.3. Section 4.4 reports our spectroscopy results concerning the membership of our variable stars. We finally summarize and conclude with Section 5.

2. OBSERVATIONS AND PHOTOMETRY REDUCTIONS

2.1. Initial Photometry Observations to Find Variables

The bulk of the photometry observations for NGC 3201 was conducted during three separate observing runs in June 1996, May 1997, and May 1998 at the Las Campanas Observatory (LCO) 1 m Swope Telescope. For all three runs Johnson-Cousins *VI* filters were used, and the number of images are approximately evenly divided between the two bands. During the June 1996 run we obtained 17 epochs (600s exposure time) using a TEK 5 CCD with 24 arcmin on the side. For both the May 1997 and May 1998 runs we used a SITe 1 CCD with 23.5 arcmin on a side (Figure 1), and obtained 164 epochs and 89 epochs (all with 600s exposure time), respectively. During the May 1998 run we took additional shorter exposures of the cluster to complete the CMD in the brighter regions (these shorter exposures were not used to detect variable candidates), as described in von Braun & Mateo (2001, BM01 hereafter).

2.2. Processing and Data Reduction of the LCO Data

The details of the IRAF² processing as well as the basic data reduction of the May 1998 data are described in BM01, section 2.1. The processing of the May 1997 and June 1996 runs was performed in the same way. All data were reduced using DoPHOT (Schechter, Mateo, & Saha 1993) in fixed position mode (see BM01) after aligning every image to a deep-photometry template image created by combining the 15 best seeing frames for each filter from the May 1998 data. The astrometric measurements, application of aperture corrections, as well as photometric calibration of the May 1998 images are outlined in BM01. All data from the other two observing runs were shifted to the coordinates and the photometric system of the calibrated May 1998 600s exposures. Since NGC 3201 suffers significant differential reddening across the field-of-view, the stars were dereddened using the differential extinction map in BM01 so that the E_{V-I} zero point applied to all stars in the field is 0.15. This differential reddening correction is applied to the data presented in Figure 3.

2.3. Additional Photometry

In order to precisely determine the times of quadrature (maximum radial velocity) for two of the variable stars we discovered (V11, the Algol, and V12, the detached system; see Section 4.1 and Figures 7 and 8), we performed additional *VI* 600s photometry observations at the Cerro Tololo Inter-American Observatory (CTIO) 0.9m Telescope during the nights of February 25 - 28, 2001, just prior to our spectroscopy follow-up CTIO 4m run (see Section 4.4). The 0.9m telescope setup included a TEK2048 CCD which provided a field-of-view of approximately 13.5 arcmin on the side (Figure 2). Initial data processing was done with the IRAF QUADPROC package. For each night, 10 bias frames were combined for the bias subtraction. Flat-field images were produced by combining five twilight flats per filter per night. The fields we observed were centered on the approximate locations of the detached candidate (Field D: $\alpha_{2000} = 10^h17^m25.72^s$ and $\delta_{2000} = -46^\circ20'12.4''$) and the Algol candidate (Field A: $\alpha_{2000} = 10^h18^m32.74^s$ and $\delta_{2000} = -46^\circ30'42.5''$). Field D fell entirely within our original field-of-view which was centered at $\alpha_{2000} = 10^h17^m36.8^s$ and $\delta_{2000} = -46^\circ20'40.0''$, whereas Field A contained stars which we had not observed previously (see Fig. 2). We secured 31 *I* and 27 *V* observations of Field A as well as 33 *I* and 35 *V* observations of Field D.

Following the publication of this work, we will make our entire photometry dataset available to readers over the Internet, using NASA's Astronomical Data Center, accessible at <http://adc.gsfc.nasa.gov>.

3. FINDING THE VARIABLE STARS

The starting point for our analysis of the LCO photometry with respect to finding binaries and determining their periods was a database which contained the data on approximately 130 observational epochs (600s exposure time) of 45000 stars in each filter per image.

3.1. Variability Detection

The criteria we set in order to extract variable star candidates from the list of stars in our database were the following:

1. χ^2 per degree of freedom, calculated based on the assumption that every star is a non-variable, has to be greater than 3.0. We furthermore set a $\sigma > 0.05$ mag threshold for a star to be taken into consideration as a variable candidate.
2. The star under investigation must appear in at least 75% of the epochs.
3. The detected variability should not be due to only a few outliers (3-5% of the datapoints) causing the high χ^2 . Care was taken to avoid deleting possible eclipsing systems at this stage (see below).
4. The star under investigation should display a brightness variation in both filters, and the variability signal should be correlated in both filters (this algorithm is very similar to the one described in Welch & Stetson (1993) and Stetson (1996)).

Any measurement of stellar magnitude was weighted by the square of the inverse photometric error associated with it. Steps 1 and 2, which were performed simultaneously, returned around 2700 (*V*) and 4500 (*I*) variable candidates. Step 3 reduced both of these numbers by approximately 50%. Step 4 further reduced the number of candidates to a total of 80 candidates. The data for these remaining candidates were then phased and inspected by eye, which is described in the next Subsection.

We note that we did not systematically address the issue of completeness in our analysis. The choice of parameters for the steps outlined above was made mainly based on hindsight (e.g., all of our candidates' χ^2 values are well in excess of 100) or trial and error (e.g., the analysis of a set of phased lightcurves before and after a reduction criterion was applied).

One set of binary star system, however, might be prone to being deleted during step 3. A detached system with a period long enough so that eclipses are not very well sampled might show up as a system whose χ^2 is based solely on a few outliers. In order to ensure that we would not miss such a system, we developed a slightly modified set of criteria specifically aimed at detecting detached binary star systems with the basic idea to identify faint "outliers" which fall next to each other in time.

1. As a first step, the mean magnitude plus standard deviation of the brightest 75% of the datapoints are calculated.
2. We now try to detect successive (in time) datapoints which are $n\sigma$ fainter than this mean magnitude. The choice of n depends on the quality of the photometry of the star in question and the number of datapoints for the star.
3. If the i -th datapoint falls within Δt of datapoint $i - 1$ (where i indicates succession in time), a merit function is calculated whose value would be $\delta_i \times \delta_{i-1}$. δ_i is defined as the magnitude difference between the i -th datapoint and the average magnitude of the 75% of the brightest stars, divided by the standard deviation (see step 1). Δt is dependent on the observing strategy followed to detect the binaries (i.e., it would be shorter, perhaps up to an hour, for a strategy where the cluster is observed many times in succession, and longer, perhaps several hours, if the cluster is observed only once every so often). It is obvious that for more than two neighboring faint outliers, the merit function would rapidly increase in value.
4. Candidates for detached systems are selected based on the value of their merit functions.

The application of this algorithm to our data revealed the existence of one detached system in our field-of-view (V11; see Section 4.1 and Figure 8) which had been eliminated by application of criteria described at the beginning of this Subsection.

3.2. Period Determination

The final decision as to whether a star is a true variable candidate (and if so, what kind of variable star it is) was based on the inspection of the phased data (the photometry lightcurve). The initial estimates of the periods of all our variable star candidates which survived the steps outlined in the previous Subsection were determined by two independent algorithms:

- the minimum-string-length (MSL) method, based on a technique by Lafler & Kinman (1965) and described in Stetson (1996).
- the Analysis of Variance (AoV) method, described, e.g., in Schwarzenberg-Czerny (1989). The basic code for this algorithm was supplied to us by Andrzej Udalski (private communication, 1998).

Both of these methods worked very well with our dataset to the extent that the periods for a variable star candidate, as independently determined by the two methods, were practically identical. A final tweaking of the precision in the period for a candidate was then done by hand, based on the appearance of the lightcurve. In the majority of the cases of the smoothly varying variables, such as W UMa stars or the RR Lyrae, the periods as determined by AoV or MSL could, in principle, not be improved by hand, i.e., the period was already determined to the maximum precision possible for our dataset. In the cases of the detached system and the Algol, we were able to increase the precision of the periods in general at the $\geq 10^{-4}$ days level. This effort helped ensure that knew the exact times of quadrature of these systems during our spectroscopic observations.

3.3. Analysis of Additional CTIO Photometry Data

In order to verify that our period estimates for the detached (V12) and Algol (V11) systems were sufficiently precise to accordingly phase our spectroscopic follow-up observations, we re-observed NGC 3201 at the CTIO 0.9m Telescope, as described in Subsection 2.3. Field A and Field D provided additional phasing information for the two binaries, enabling us to improve our period estimates for both of these systems. In the case of the detached system, this correction was on the order of five seconds, whereas the previously calculated period for the Algol system proved to be off by less 0.2 seconds.

Field A furthermore contained stars we had not observed in our previous monitoring program, giving us the chance to mine additional data of NGC 3201 for the existence of variable stars. Using the algorithms described above, we detected three additional W UMa systems outside our previous field of view (V7-9; see Figures 1 and 2). We made use of the fact that we had repeated V and I observations of the same system (the Algol star) in both the CTIO and the LCO datasets to photometrically shift the CTIO data to the system of the LCO data. The differential dereddening of the CTIO dataset W UMa variables (V7-9) was performed as described above and in BM01.

4. RESULTS

4.1. Locations of Variable Stars in Field and in CMD

Table 1 gives the basic information about the variable stars we detected in the field of NGC 3201. V_{bright} and I_{bright} are the V and I magnitudes at maximum light, respectively. Figure 1 shows the locations of the variable stars in the LCO dataset. Figure 2 shows the locations of V11 (the Algol) and the three additional W UMa systems we found in the CTIO photometry data. Finally, Figure 3 indicates where the variables fall within the CMD of NGC 3201. The data shown in Figure 3 are differentially dereddened to a fiducial region within the cluster, as described in BM01. No reddening zero point is applied.

4.2. Photometry Lightcurves

The phased lightcurves for the W UMa systems V1 through V5, detected in the LCO dataset, are presented in Figure 4. The three additional W UMa lightcurves, V7 through V9, extracted from the CTIO photometry data (note the difference in sampling due to the lower number of observational epochs for these stars), are in Figure 5, along with the lightcurves of V10, the RR Lyrae, and V13 and V14, the two unclassified systems, from the LCO dataset. Figure 6 contains the lightcurve of V6, the only member of NGC 3201 among our set of variable stars. V11, the Algol system, and V12, the detached system, are presented in Figures 7 and 8, respectively. In all of these three Figures, V data are in the bottom panel, I data in the top panel. The error bars represent the photometric errors associated with that particular measurement of the star's magnitude. No reddening correction was applied to the lightcurves.

4.3. Rucinski Magnitudes

W Ursa Majoris binaries are systems in which the two components are in physical contact with their Roche equipotential lobes and at their inner Langrangian Point (see Mateo (1993), Rucinski (1985a), and Rucinski (1985b) for more detailed descriptions of W UMa systems). Due to the good thermal contact between the two components, the two stars are assumed to have the same surface temperature. The total luminosity of the system can therefore be defined as (Rucinski 1995; Mateo 1996)

$$L = KT^4 S(q, P, f) M_p^{\frac{2}{3}} (1 + q)^{\frac{2}{3}} P^{\frac{4}{3}}, \quad (2)$$

where K consists of well-known constants, T is the common surface temperature, M_p and M_s are the masses of the primary and secondary component, respectively, $q = M_s/M_p$, and P is the orbital period of the system. S represents the total stellar surface area as defined by the Roche geometry, dynamical properties of the binary, and the fill-out factor f by which the stellar surfaces extend beyond the inner critical Roche surface.

Rucinski (1994, 1995, 2000) converted the above equation into the more convenient form

$$M_V^{color} = a_0 + a_1 \log P + a_2 color, \quad (3)$$

where M_V is the absolute V magnitude, P is the period in days, and the color is reddening-free. For $V - I$ color, this equation is (Rucinski 2000)

$$M_V^{VI} = -4.43 \log P + 3.63(V - I)_0 - 0.31; \sigma \sim 0.29. \quad (4)$$

Table 2 shows the thus calculated absolute magnitudes and distance moduli for the W UMa binaries in the field of NGC 3201. The distance to NGC 3201 was calculated in BM01 to be 4.5 ± 0.03 kpc; the value found in Harris (1996) is 5.2 kpc. The corresponding distance moduli are $V_0 - M_V = 13.58$ and 13.26, respectively.³ We note that the absolute magnitudes and distance moduli in Table 2 were calculated under the assumption that the W UMa system under investigation is suffering the full extinction between us and the cluster. Since the spectroscopy results indicated that no W UMa system except V6 is associated with NGC 3201 (see following Subsection), and the Rucinski magnitudes for some of the variables indicate that they are foreground stars, this assumption might be incorrect in some cases. That is, for some of the non-members, the color might not be the correct, reddening-free value.

The distance modulus of the GC member V6 calculated in Table 2 is 13.873, larger than the NGC 3201 distance moduli in both BM01 (by $\sim 2\sigma$) and Harris (1996) (by $\sim 1\sigma$). One way to “force” V6 to be at the correct distance would be to change the reddening zero point to the cluster and thus change the variable’s intrinsic color. Since this correction would force the distance to go down, the reddening zero point obtained this way would decrease to $E_{V-I} \sim 0.02$, significantly below the BM01 value of 0.15. At this point, we can therefore not offer any conclusive reason why V6’s distance modulus is slightly too high, other than the possibility that this one particular binary would represent an outlier (by about 1-2 σ) in Rucinski’s empirically determined relation.

4.4. Cluster Membership

A first indication of whether an eclipsing binary star system in the field of a globular cluster is associated with that cluster is, of course, its location with respect to the cluster center (we note that we cannot study the very center of the cluster due to crowding). The tidal radius of NGC 3201 is 28.45 arcmin (Harris 1996). Thus, all the binary systems we find are well within the tidal radius. A more powerful membership criterion is a binary’s location in the CMD. Based on the CMD of NGC 3201 (see Figure 3), V5, V7, V8, V10, V13 and V14 are not associated with the cluster. Furthermore, based on their distance moduli, the W UMa systems V3, V4, V5, and V8 seem to be foreground stars while V9 seems to be a background star. V1, V2, and V6, however, seem promising cluster member candidates within error estimates, with the only difference being that the reddening calculated for V1 and V2 is significantly lower than the one for V6 (see Table 2).

The final verdict on membership, however, can only be provided by spectroscopic observations. NGC 3201 has a distinct systemic (retrograde) velocity of approximately 500 km/s (Harris 1996; Côté et al. 1994), so a single spectrum of a binary system with sufficient resolution and signal-to-noise ratio can be used to establish cluster membership.

During the nights of March 2 - 5, 2001, we performed spectroscopic follow-up observations of our eclipsing bi-

nary star candidates at the CTIO 4m Telescope with Arcon and the RC Spectrograph. Our setup included a 3k x 1k Loral CCD and the KPGLG grating (860 l/mm; 1st order blaze = 11000 Å) in second order. The wavelength coverage extended from 3800 to 5100 Å, with a resolution of about 0.4 Å/pixel. Our observing targets were V1, V2, V3, V4, V6, V11 and V12. V9, a potential cluster member given its location in the CMD, was too faint to observe with our setup at CTIO.

In order to check the cluster membership of V9, we obtained three spectra during the night of March 19, 2001, using the Magellan 1 Telescope with the Boller & Chivens Spectrograph and a setup similar to the one at the CTIO 4m Telescope but with lower resolution (approximately 1.4 Å/pix). Our wavelength coverage extended from 3900 to 5300 Å.

To our great disappointment during the first night of the CTIO spectroscopy run, one spectrum after the next eliminated our candidates from cluster membership consideration. The only system with a systemic velocity equal to that of NGC 3201 is V6, a blue straggler candidate (see Figure 3) with a very small amplitude (see Figure 6).

Our spectroscopy results are summarized in Table 3. The systemic velocities of the binaries were determined using the IRAF FXCOR package, using radial velocity standards as templates. We estimate our error in the velocity determinations of the candidates to be around 20 km/s for the CTIO data (except V6), based on measurements performed on the velocity standards we used. Due to the lower resolution of the spectrum we obtained at Magellan, we estimate V9’s velocity uncertainty to be approximately 50 km/s. The difference in spectral types between V6 and our radial velocity standards made it impossible to determine its velocity using FXCOR. Instead, we calculated its Doppler velocity from line profile fitting using IRAF’s SPLIT package. The error quoted for that star is simply the rms of ~ 10 individual line measurements from different spectra of the star.

We further note that for all of our variables, except for our CTIO photometry targets (V7-9 as well as V11 and V12), we do not have phase information obtained more recently than three years prior to the spectroscopy run. The propagation of the period determination error (see Tables 1 and 2) therefore makes it impossible to constrain the precise phasing of most of our candidates. The uncertainty in the calculation of the systemic velocities of the binary candidates due to the radial motion of the two components is not accounted for in our estimates.⁴

Since NGC 3201’s systemic velocity is so high (500 km/s), cluster membership based on the comparison between systemic velocity of the variable and the cluster may be determined without phasing information. The velocity amplitudes of the components of a binary system relate to the masses and the period of the system as follows (Paczynski 1996):

$$\frac{K_1 + K_2}{\sin i} = 386.4 \text{ km s}^{-1} \left(\frac{M_1 + M_2}{3M_{\text{solar}}} \frac{0.5 \text{ days}}{P_{\text{orb}}} \right)^{\frac{1}{3}}. \quad (5)$$

³ These values represent the apparent distance moduli corrected for extinction.

⁴ A binary’s period may, of course, also be calculated from the radial velocity curve. Since we were able to eliminate our observing targets (except V6) from cluster membership consideration after obtaining only a few spectra for each system, we refrained from re-observing them and can therefore not determine the phase of the binary at the time of observation.

If one assumes that the orbits of the W UMa systems V1-4 and V9 are circular (which is evidenced by the fact that the minima of the lightcurves are separated by half a period), that $\sin i = 1$ (the system is seen edge-on), and that the masses and thus velocity amplitudes of the two components are equal, one needs only the sum of the masses and the orbital period to get an estimate of the velocity amplitudes. From the isochrones of D. Vandenberg 2000 (private communication; based on evolutionary models by Vandenberg et al. (2000)) for a cluster age of anywhere inbetween 14 and 18 Gyrs and $[\text{Fe}/\text{H}]=-1.41$, one obtains masses for main-sequence stars of $(V - I)_0 \sim 0.7$ of approximately $0.7 M_{\text{Solar}}$ (for each component). Finally, given the average period of these systems of ~ 0.36 days, we estimate the typical velocity amplitude to be $K_j \sim 165 \text{ km s}^{-1}$. We note, of course, that non-member binaries might have a different metallicity and thus mass for a given color, but since $K \propto M^{1/3}$, this difference would not significantly alter this rough estimate. A deviation from an edge-on configuration would decrease the calculated velocity amplitudes, i.e., the value given above may be regarded as an upper limit.

For V11 and V12, the masses of the individual components are probably slightly larger (bluer $V - I$ color), but the periods are much larger, especially in the case of V12. Retaining the same assumptions as for the W UMa systems, one obtains velocity amplitudes closer to 150 km/s for V11, and 80 km/s for V12.

In order to for a binary system to be a member of NGC 3201, its systemic velocity would have to fall within $(165 \text{ km/s} + \sigma)$ of 500 km/s (NGC 3201's velocity). As one may easily see in Table 3, only V6 survives this criterion.

We obtained approximately 25 spectra of V6 at various phase angles. These results, combined with our photometry data, may be used to calculate the component masses of the binary BS system. The analysis of the radial velocity curve and subsequent calculation of the stellar masses will be addressed in a future publication.

5. SUMMARY AND CONCLUDING REMARKS

The low-latitude GC NGC 3201 was probed for the existence of photometrically variable stars in the magnitude range of approximately $16.5 < V < 20$ and for periods between roughly 0.2 and 5 days. We detected 14 variable

star candidates in the field of which most are eclipsing binaries of the W UMa type. Our spectroscopic follow-up observations revealed that only one of the variables, a BS W UMa EB, is associated with the cluster itself. Due to the low-latitude location of the GC, the high contamination of Galactic disk stars in the field of NGC 3201 seems to have manifest itself 13 times in our analysis.

Our confirmation of V6 as a member increases the number of known binary BSs in GCs. Mateo et al. (1990) predicted that 3%-15% of all BSs in GCs should be photometrically observable binaries. In the case of NGC 3201 there are nine total BSs (Sarajedini 1993). Our detection of one BS member binary is therefore consistent with that prediction. Thus, the membership of V6 supports the basic Mateo et al. (1990) model that BSs evolve from primordial or, at least, long-lived binaries which coalesce after a lifetime of slow angular momentum loss.

Despite the fact that we did not identify a large number of NGC 3201 member binaries, we have nevertheless shown the potential to do just that for the other globular clusters in our survey (provided there are binaries in those clusters). The fact that we successfully identified a BS EB with an V amplitude of around 0.07 mag (see Figure 6), a detached system with duty cycle of around 0.1 (see Figure 8), and that we determined periods to a precision of seconds or less (see Section 3.3) gives us confidence that we have the dataset and the methods to detect a number of EBs in our target GCs. Using the combination of our 1m telescope photometry dataset and the capabilities of Magellan 1 for the spectroscopy follow-up observations, we should be able to determine the cluster membership for binaries in the southern and equatorial GCs of our sample in the near future.

This research was funded in part by NSF grants AST 96-19632 and 98-20608. We would like to thank A. Udalski for his help with the AoV algorithm. We would also like to express our most sincere gratitude to the support staff and night assistants at CTIO, Magellan, and especially LCO without whose help and determination these observations would not have been able to produce the results presented here. Finally, we thank the anonymous referee for his/her thorough analysis of the manuscript and insightful comments and suggestions.

REFERENCES

- Andersen, J. 1991, *A&A Rev.*, 3, 91
 Bertelli, G., Bressan, A., Chiosi, C., Fagotto, F., & Nasi, E. 1994, *A&AS*, 106, 275
 Clement, C. M., Muzzin, A., Dufton, Q., Ponnampalam, T., Wang, J., Burford, J., Richardson, A., Roseberry, T., Rowe, J., & Sawyer-Hogg, H. 2001, to appear in *AJNov 2001 issue* (astro-ph/0108024)
 Côté, P., Welch, D. L., Fischer, P., Da Costa, G. S., Trambly, P., Seitzer, P., & Irwin, M. J., 1994, *ApJS*, 90, 83
 Harris, W. E. 1996, *AJ*, 112, 1487
 Hut, P. 1993, in *ASP Conf. Ser. Vol 53, Blue Stragglers*, ed. R. E. Saffer, p. 44
 Hut, P., McMillan, S., Goodman, J., Mateo, M., Phinney, E. S., Pryor, C., Richer, H. B., Verbunt, F., & Weinberg, M. 1992, *PASP*, 104, 981
 Laffer, K., & Kinman, T. D. 1965, *ApJS*, 11, 216
 Leonard, P. J. T., & Linnell, A. P. 1992, *AJ*, 103, 1928
 Livio, M. 1993, in *ASP Conf. Ser. Vol 53, Blue Stragglers*, ed. R. E. Saffer, p. 3
 Mateo, M. 1993, in *ASP Conf. Ser. Vol 53, Blue Stragglers*, ed. R. E. Saffer, p. 74
 Mateo, M. 1996, *ASP Conference Series, Vol. 90, The Origins, Evolution, and Destinies of Binary Stars in Clusters*, eds. E. F. Milone and J.-C. Mermilliod, page 21
 Mateo, M., Harris, H. C., Nemeč, J., & Olszewski, E. O. 1990, *AJ*, 100, 469
 McVean, J. R., Milone, E. F., Mateo, M. & Yan, L. 1997, *ApJ*, 481, 782
 Paczynski, B. 1996, invited talk presented at STScI
 Rubenstein, E. P. 1997, *PASP*, 109, 933
 Rucinski, S. M. 1985a, in *Interacting Binary Stars*, eds. J. E. Pringle & R. A. Wade, Cambridge, Cambridge University Press, p. 85
 Rucinski, S. M. 1985a, in *Interacting Binary Stars*, eds. J. E. Pringle & R. A. Wade, Cambridge, Cambridge University Press, p. 113
 Rucinski, S. M. 1994, *PASP*, 106, 462
 Rucinski, S. M. 1995, *PASP*, 107, 648
 Rucinski, S. M. 2000, *AJ*, 120, 319
 Sarajedini, A. 1993, in *ASP Conf. Ser. Vol 53, Blue Stragglers*, ed. R. E. Saffer, p. 14
 Sawyer-Hogg, H. 1973, *Publ. Dom. Astrophys. Obs. Victoria*, 3, 6

Schechter, P. L., Mateo, M., & Saha, A. 1993, *PASP*, 105, 1342
Schwarzenberg-Czerny, A. 1989, *MNRAS*, 241, 153
Sills, A., & Baily, C. D. 1999, *ApJ*, 513, 428
Sills, A., Baily, C. D., Edmonds, P. D., & Gilliland, R. L. 2000,
ApJ, 535, 298

Stetson, P. B. 1996, *PASP*, 108, 851
VandenBerg, D., Swenson, F., Rogers, F. J., Iglesias, C. A., &
Alexander, D. R. 2000, *ApJ*, 532, 430
von Braun, K., & Mateo, M. 2001, *AJ*, 121, 1522
Welch, D. L., & Stetson, P. B. 1993, *AJ*, 105, 1813

TABLE 1
VARIABLE STARS IN THE FIELD OF NGC 3201

Var. No.	type	RA (2000)	Dec (2000)	period (days)	V_{bright}	I_{bright}
V1	W UMa	10:16:36.92	-46:22:29.3	0.303587(28)	18.054(17)	17.258(20)
V2	W UMa	10:17:07.73	-46:30:18.2	0.345095(42)	18.237(14)	17.319(19)
V3	W UMa	10:17:13.75	-46:27:54.7	0.377114(43)	17.189(21)	16.352(21)
V4	W UMa	10:17:17.18	-46:27:37.5	0.44179(55)*	16.850(17)	15.965(22)
V5	W UMa	10:17:52.93	-46:34:06.7	0.276216(31)	19.847(21)	18.380(32)
V6	W UMa	10:17:59.08	-46:33:25.7	0.37307(39)*	17.270(13)	16.599(19)
V7	W UMa	10:18:56.03	-46:36:10.4	1.0800(90)	18.658(15)	17.064(19)
V8	W UMa	10:18:46.01	-46:30:13.8	0.30642(75)	18.824(14)	17.577(19)
V9	W UMa	10:18:31.97	-46:37:32.9	0.33248(61)	19.609(22)	18.483(27)
V10	RR Lyrae	10:18:03.86	-46:17:48.7	0.592920(53)	17.088(12)	16.446(22)
V11	Algol	10:18:32.74	-46:30:42.5	0.702127(99)	17.728(13)	16.932(19)
V12	Detached	10:17:25.72	-46:20:12.4	2.84810(98)	17.225(14)	16.301(22)
V13	Unclass. 1	10:17:04.83	-46:26:39.7	1.2080(44)*	20.203(35)	18.529(29)
V14	Unclass. 2	10:18:36.28	-46:22:06.2	2.160(13)*	18.915(16)	17.108(21)

Note. —

- Errors in parentheses indicate the uncertainty in last two digits, i.e., $0.303587(28) = 0.303587 \pm 0.000028$ and $2.160(13) = 2.160 \pm 0.013$.
- Photometry errors are the result of adding in quadrature the DoPHOT photometry error for the instrumental magnitude and the rms of the standard star solution (see BM01).
- The error in the period corresponds to the full width at half maximum (fwhm) of the peak in the AoV power spectrum corresponding to the correct frequency. For the determination of this error, only V data were used, except for the cases of V7, V8 and V13 where we used I data. In some instances, the peak in the power spectrum corresponding to the correct period was assigned essentially the same power as directly neighboring peaks (i.e., it would be hard to pick “by eye” which one is the correct one). In these cases, we estimated the period error to be the distance between the two neighboring peaks (with the peak corresponding to the correct period in the middle). These cases are marked by an asterisk.

TABLE 2
RUCINSKI MAGNITUDES AND DISTANCE MODULI FOR W UMA-TYPE BINARIES

system	period (days) ^a	E_{V-I} ^b	$(V-I)_{0,bright}$ ^c	$M_V(Rucinski)$	$V_0 - M_V$
V1 ^d	0.303587(28)	0.131(55)	0.665	4.397	13.405
V2	0.345095(42)	0.202(34)	0.716	4.336	13.513
V3	0.377114(43)	0.183(38)	0.654	3.940	12.898
V4	0.44179(55)	0.183(38)	0.702	3.810	12.689
V5	0.276216(31)	0.305(65)	1.162	6.383	12.878
V6	0.37307(39)	0.366(42)	0.305	2.694	13.873
V7	1.0800(90)	0.352(81)	1.242	4.050	13.932
V8	0.30642(75)	0.275(61)	0.972	5.494	12.802
V9	0.33248(61)	0.368(67)	0.758	4.560	14.343

^aAs in Table 1, errors in parentheses indicate the uncertainty in last two digits. The period errors are the same as in Table 1.

^b E_{V-I} contains the reddening zero point, calculated in BM01 to be 0.15 mag. As mentioned above, this value assumes that the binary suffers the full extinction along the line of sight to the GC (which is not necessarily correct if the binary is not a cluster member). The errors for E_{V-I} are the random errors in the determination of the *differential reddening*. That is, a possible systematic error in the determination of the reddening zero point (described in BM01) is not included in this estimate.

^c $(V-I)_{0,bright}$ is the dereddened color at maximum light.

^dV1 is located in a region whose differential reddening along the line of sight is lower than the one of the fiducial region whose overall E_{V-I} is 0.15 mag. Its total E_{V-I} is therefore calculated to be lower than the reddening zero point.

Note. — Rucinski quotes the scatter in his relation (Rucinski 1994, 1995) to be 0.29 mag in the calculation of the absolute V magnitudes (corresponding to an uncertainty of approximately 13% in distance). Since this uncertainty is far larger than the quadratic sum of all our random errors, we refrain from a detailed error analysis for the Rucinski magnitudes and distance moduli.

TABLE 3
SYSTEMIC VELOCITIES OF MEMBER CANDIDATES

variable	systemic velocity (km/s)	error (km/s)
V1	12	20
V2	6	20
V3	9	20
V4	20	20
V6	513	44
V9	24	50
V11	1	20
V12	0	20

Note. —

- The variables not listed in this table but listed in Tables 1 and 2 were considered to be non-members based on their location in the CMD.
- For an explanation on how velocities and errors were determined, see text.
- The systemic velocity of NGC 3201 is $\sim 500 \text{ km/s}$ (Harris 1996; Côté et al. 1994).

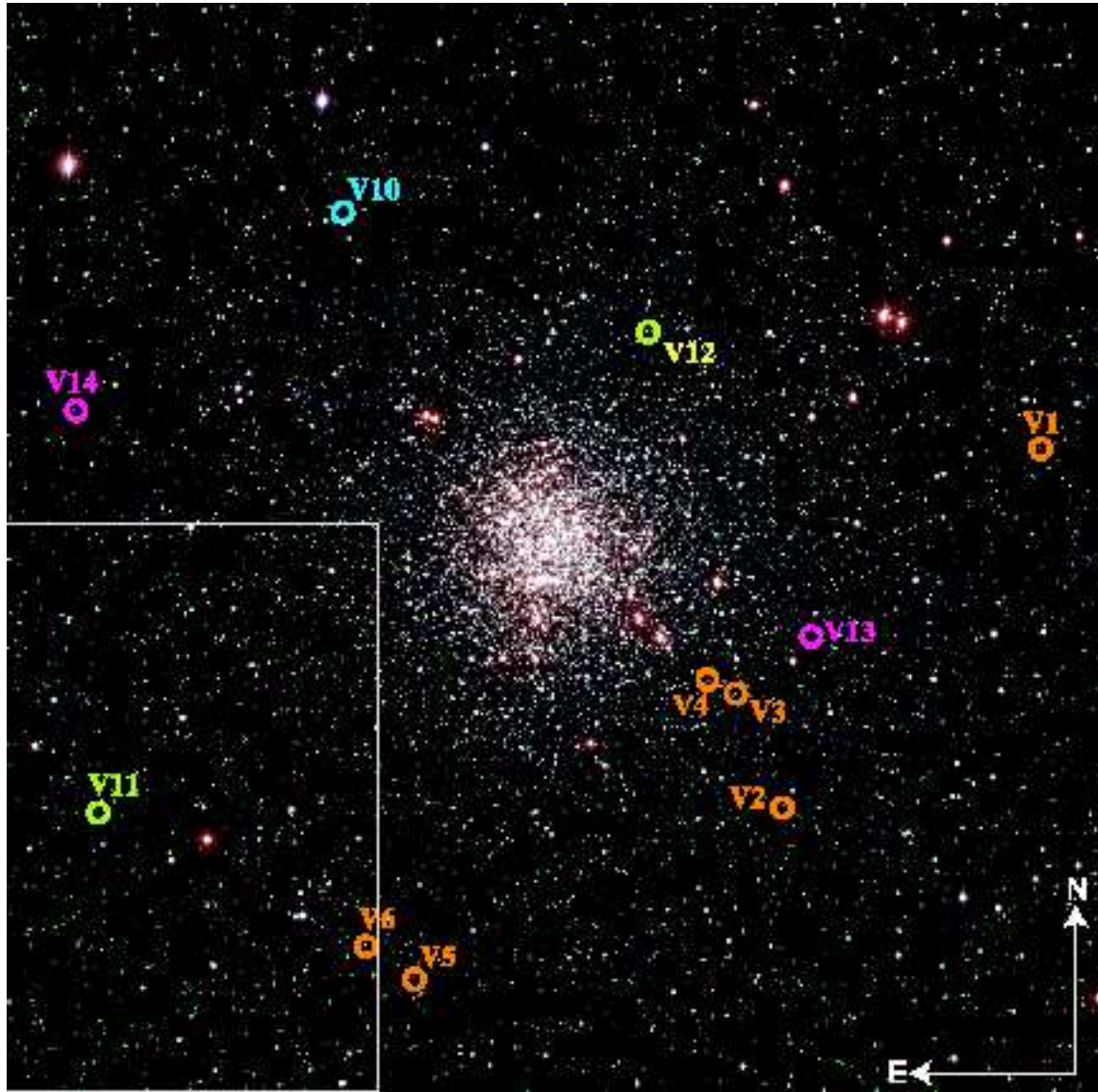


FIG. 1.— The locations of the variable stars in the LCO data. The field-of-view is 23.5 arcmin on the side. North is up and east is to the left. The rectangle toward the bottom left part of the figure represents the approximate boundaries of the overlap region of this Figure and Figure 2, i.e., the north-west part of Figure 2.

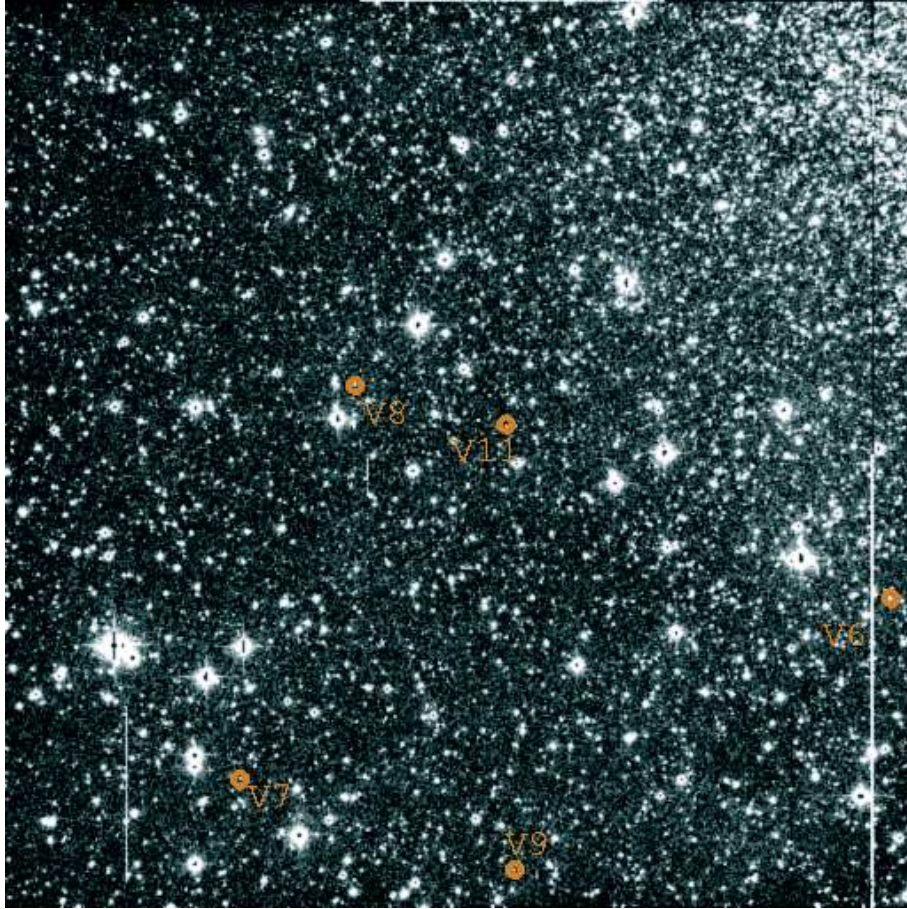


FIG. 2.— The locations of the variables extracted from the CTIO 0.9m data. The field-of-view has the same orientation as the one in Figure 1, but is smaller (13.5 arcmin on the side in this figure). V11, toward the center of this image, and V6, toward the right edge of the image, are present in both fields-of-view. V7-9 are located outside (south-east of) the field of Figure 1.

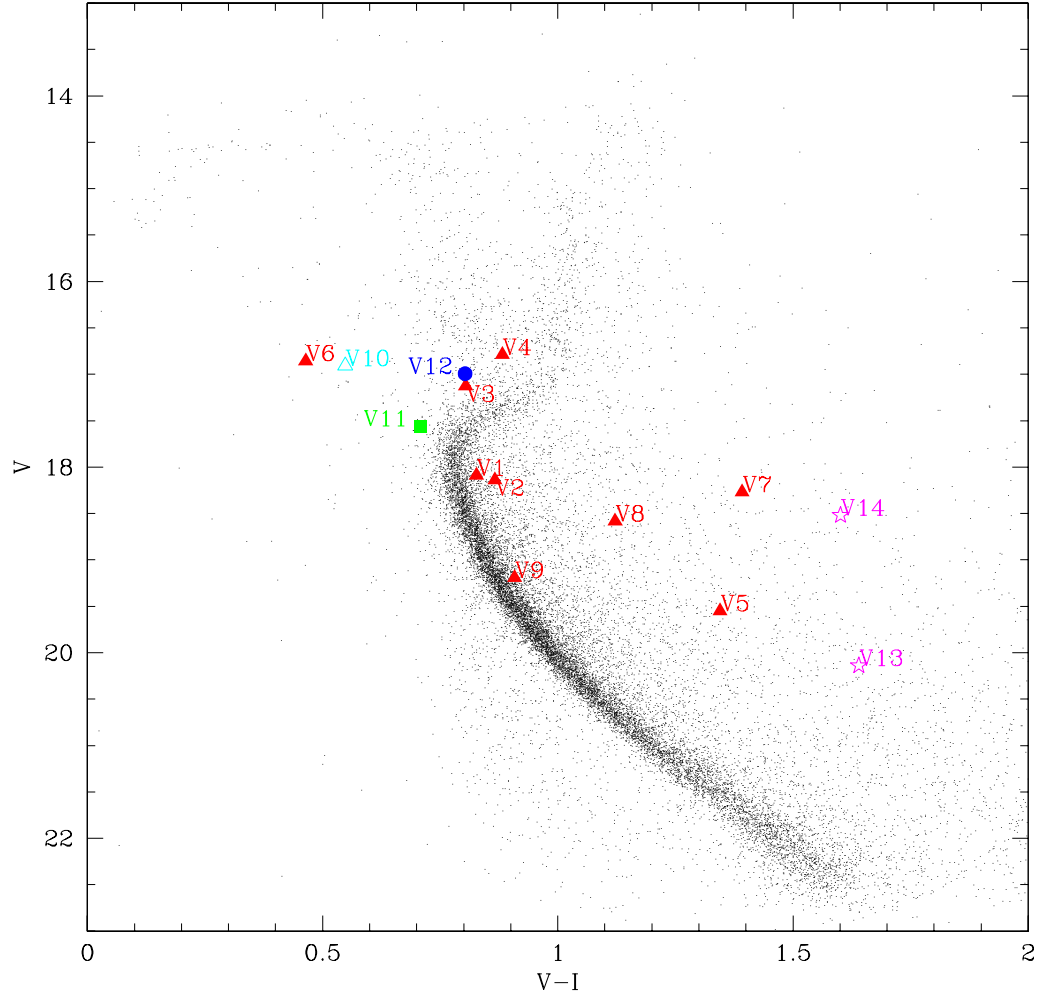


FIG. 3.— The locations of all our variable stars in the field of NGC 3201 in its CMD. The data presented are differentially dereddened to the fiducial region defined in BM01, i.e., no reddening zero point is applied. In BM01, we calculate the E_{V-I} zero point to be 0.15. The variable stars are plotted at maximum brightness and are also differentially dereddened. Filled triangles represent W UMa types, the open triangle the RR Lyrae, the square the Algol system, the filled circle the detached system, and the open star-shaped symbols the unclassified systems.

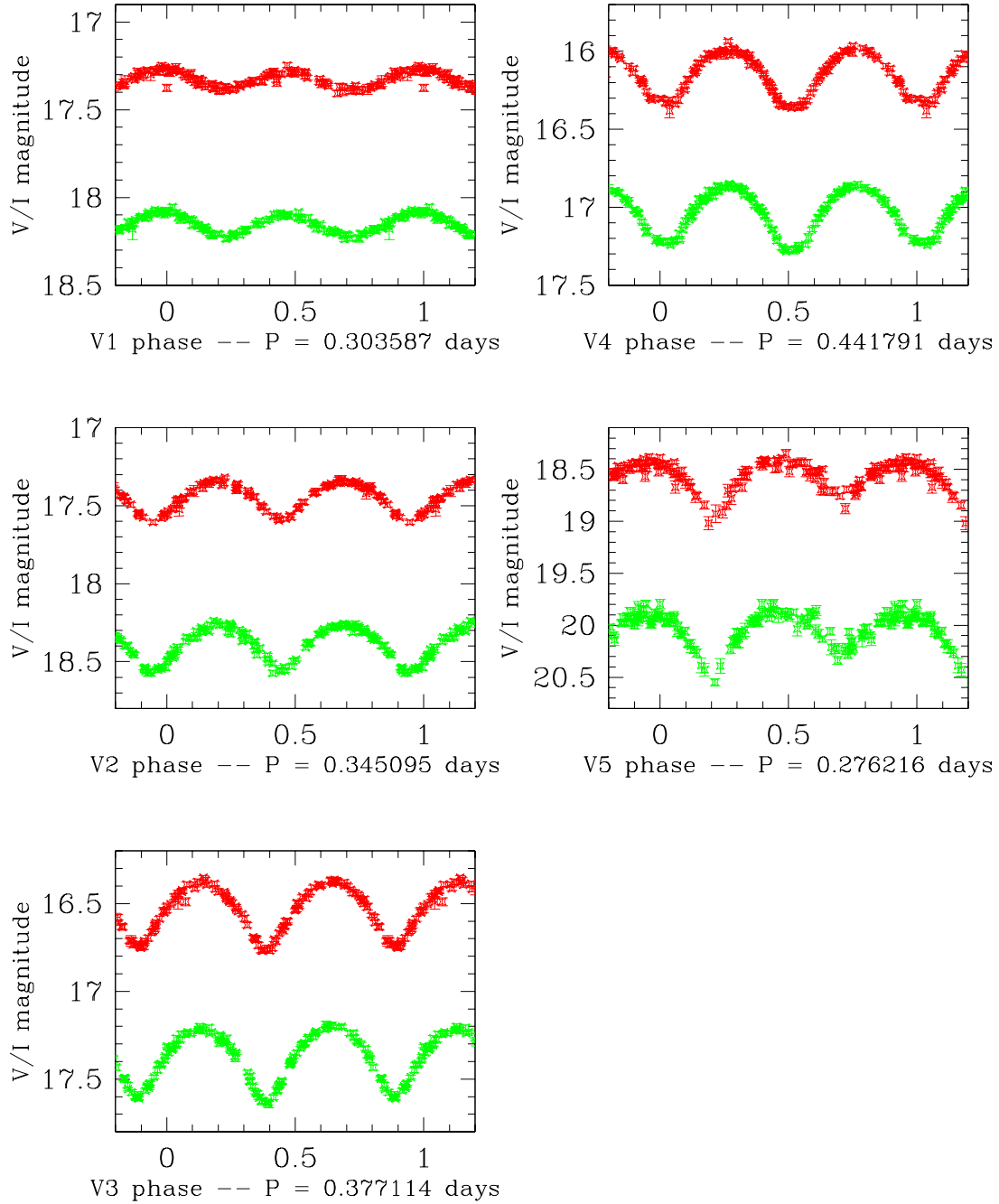


FIG. 4.— The V and I lightcurves of V1 through V5 (all W UMa type binaries). I magnitude is the upper curve in each of the panels; no extinction correction is applied. None of these variables is associated with NGC 3201 itself.

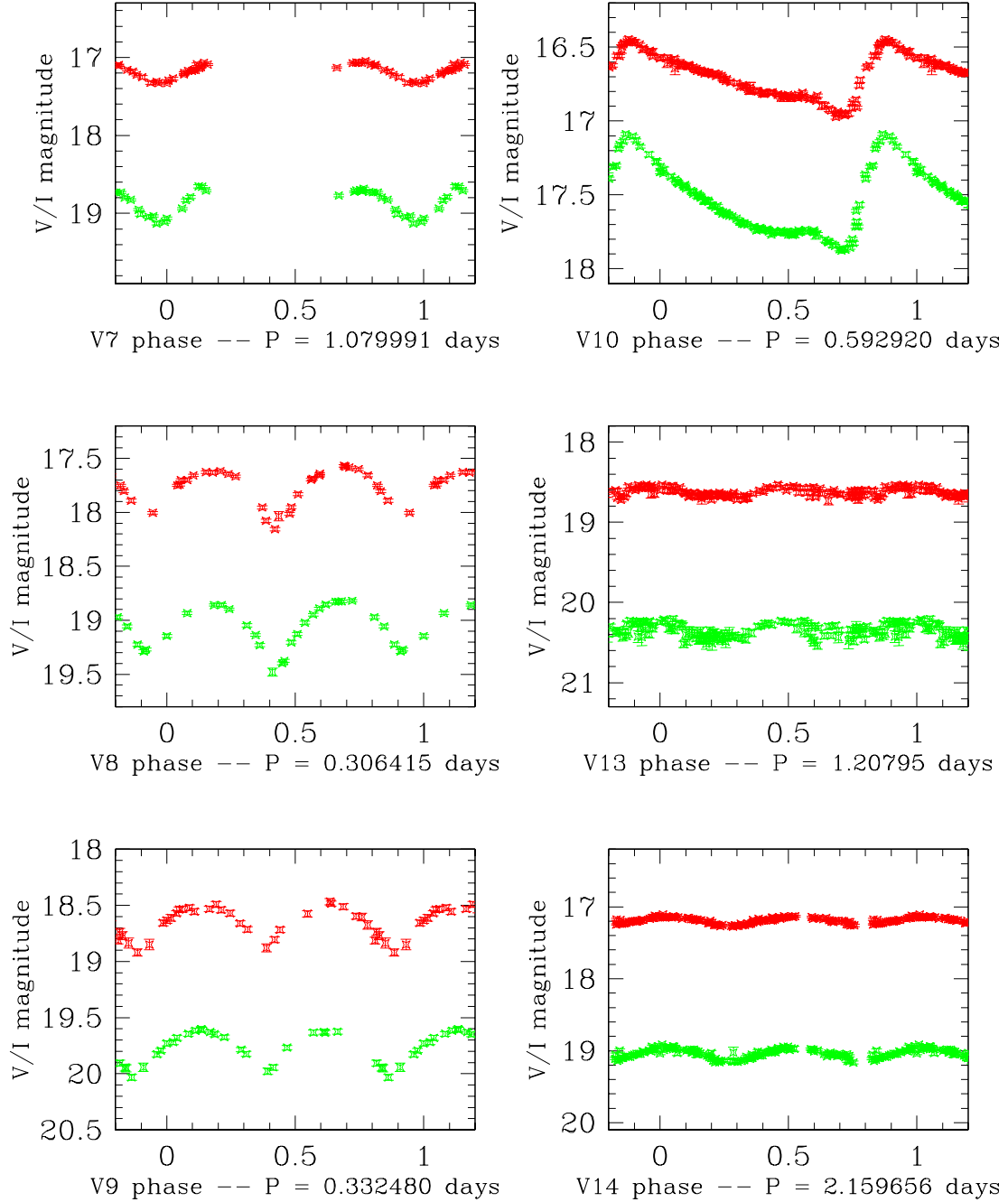


FIG. 5.— V7-V9 are the W UMa systems discovered in the CTIO dataset. Note the much sparser sampling of the lightcurves. V10 is the background RR Lyrae star. Finally, V13 and V14 are the two unclassified systems. Their lightcurves look similar to the W UMa types, but their periods are much longer and their colors much redder. In each panel, the I magnitude is plotted above the V magnitude. The data are not corrected for extinction.

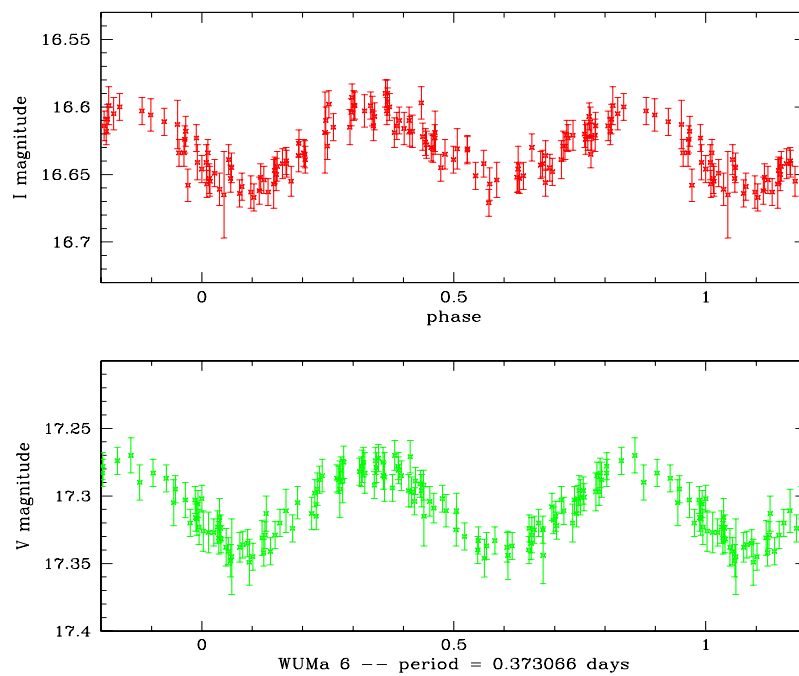


FIG. 6.— The lightcurve of V6, a blue straggler candidate and the only variable star in our sample which is a member of NGC 3201. No extinction correction is applied.

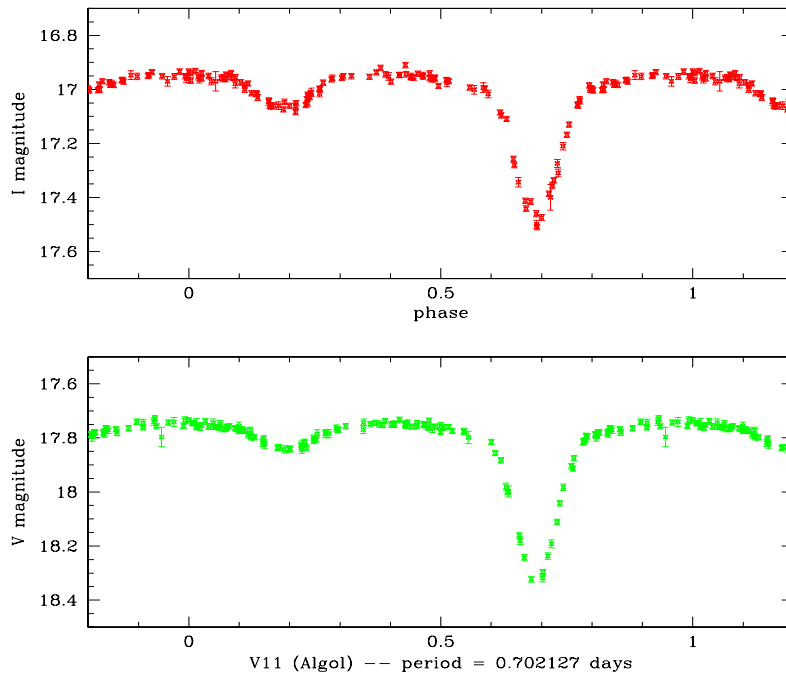


FIG. 7.— The lightcurve of V11, the Algol system, comprised of data taken at both LCO and CTIO. No reddening correction is applied to the data. V11 is not a member of the globular cluster.

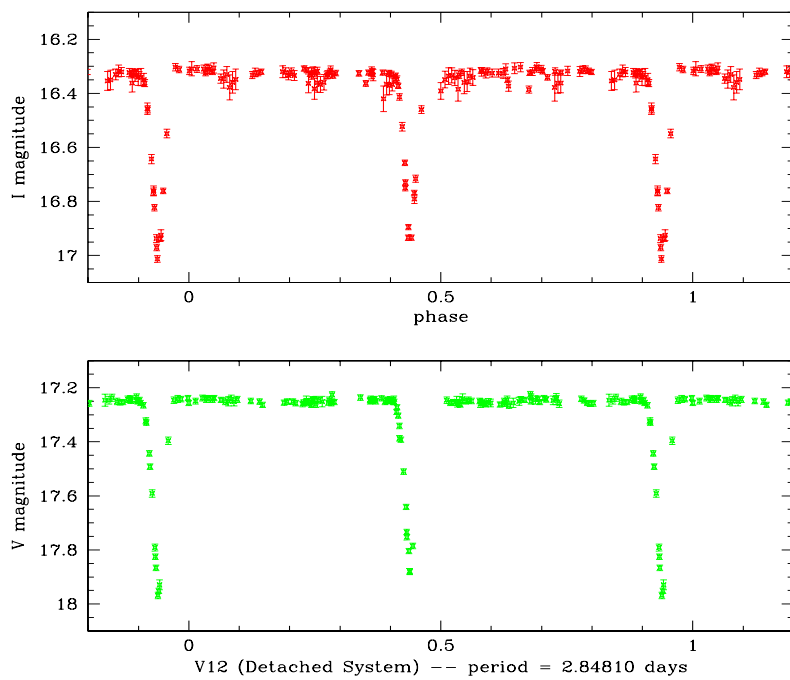


FIG. 8.— The lightcurve of V12, a detached binary star system. The data for this lightcurve were taken both at LCO and CTIO, and they are not corrected for extinction. V12 is not associated with NGC 3201.